Journal of Engineering Science and Technology
Vol. 15, No. 4 (2020) 2507 - 2521

SIMULATION ON DRYING OF SAGO BAGASSE IN A FLUIDIZED BED DRYER

TANTIYANI N. A. OTHMAN*, ZAIDI A. M. DIN, SOBRI M. M. TAKRIFF

Department of Chemical and Process Engineering, Faculty of Engineering and Built Environment, Universiti Kebangsaan Malaysia, 43600, Bangi UKM, Selangor, Malaysia
*Corresponding Author: tantiyani@ukm.edu.my

Abstract

Sago from species of *Metroxylon Sago* is widely grown in Malaysia, especially in Sarawak. With the rapid growth of sago starch production, it produces a lot of waste that needs to be managed systematically. Various methods are being undertaken to manage sago's waste including converting it to the high-value products such as animal feeds by a drying mechanism. Some of the widely used of drying methods are solar drying, microwave drying, heat pump and fluidized bed dryer (FBD). Among them, FBD shows some advantages with high energy efficiency, has high mass transfer rates and drying rates as well as has a shorter drying time. These advantages have made it to be very practical used for application in the food industry in producing great quality dried food products such as fruits, vegetables and cereals. Due to that reason, the drying of the sago bagasse in the FBD was studied by a computational fluid dynamic modelling as it can be executed in a short period of time as compared to the experimental approach. In this study, a horizontal FBD which is the most effective and widely used as a dryer has been developed in the ANSYS© Fluent 19.2 software and a simulation is carried out with Euler-Euler multiphase model to observe the drying profile inside the FBD. The simulation was studied at different temperatures of 50, 70 and 100°C with varying inlet velocities of 5, 8 and 10 ms^{-1}. The simulation results show the higher inlet temperature and velocity will result in the greater drying rate and shorter drying time. To achieve the shorter drying time in the FBD, the temperature of 70°C and hot air velocity of 10 ms^{-1} was found to be the optimum condition for sago drying. Besides, it was observed the weight percentage of water in the sago bagasse decreases from 40% to 15.7%, 17.79% and 20.21% at T = 50, 70 and 100°C, respectively. The moisture content in the outlet of the sago bagasse was within the range of 15-20% which is suitable for the production of animal feed.

Keywords: Drying, Euler-Euler CFD, Fluidized bed dryer, Sago Bagasse.

1. Introduction

Sago from species of *Metroxylon Sago* is widely grown in Malaysia, especially in Sarawak. It has become one of the most important commodities and it is extensively planted with estate plantation scheme introduced to farmers in Sarawak. Sago trees can be classified as multi-purpose trees and sago starches are the most important product of sago trees. It can grow up to 9 to 14 years and the starch is accumulated in the pith until the full-blooming season stage [1]. Aside of Indonesia and Papua New Guinea, Malaysia becomes the third world sago starch producer with the contribution of 94.6% combined production. A matured sago tree would grow tall from 7 to 15 m with the average diameter of 120 cm.

The pith of palm contributes utmost of the starch. It contains approximately 250 kg of starch, 425 kg of water and 175 kg of other material [2]. Pei-Lang et al. [2] found the sago pith contains 6-12% dissolved solids, 1-2% ash and 79-88 % sugar and starch. The starch from the sago trees has variety of uses in many industrial applications; in food and non-food industries. It can be utilized in the bio-technology, animal feed and others [3, 4]. There are many uses of sago in the non-food industries [5]. In addition, sago can be also used as an adsorption material for heavy metals such as mercury [6], as sugar syrup and energy source for biomass [7] and many other applications. Besides, the sago pith also consists of other materials such as fibre, hemicellulose and other untraced substances. It may be slightly different according to the stage of the growth. Liestianty et al. [8] conducted a series of test on a few samples of treated sago starch and concluded that the starch still contains 13.66-15.80% of water. The high percentage of water content will easily damage the starch as it can lead to fungal growth and flea attack. Thus, the drying process of starch become crucial and important to ensure the quality of the product.

Nowadays, there are many types of drying technologies applied in the food industries. Some of the widely used methods are solar drying, microwave drying, heat pump and fluidized bed dryer (FBD). Each of these drying methods has its own advantages and disadvantages and one method is suitable for certain applications. Although there are many types of the drying technology used in food industry, the most effective and widely used for drying method is FBD [9, 10]. It is because the FBD can enhance rapid mixing with uniform temperature and concentrations, resisting the rapid temperature changes, and hence, it would respond slowly to changes in operating conditions and prevent the temperature runaway occurrence with exothermic reactions [10]. Besides, FBD has an ability to circulate solids between fluidized beds for heat exchange, can achieve good heat and mass transfer rates as well as it is applicable for either large- or small-scale operations. These advantages have made it to be very practical to be used for application in the food industry in producing great quality dried food products [11, 12].

Numerous studies on the drying in the FBD are reported in the food and non-food industries. For example, Arumuganathan et al. [13] analysed the drying of mushroom in the FBD and they found that the temperature of a hot air feed has an effect to the rate of drying. Also, they achieved the optimum temperature for the mushroom's drying was at 60°C. In addition, Mortier et al. [14] analysed the behaviour of drying profile of a wheat grains in the FBD to predict the temperature and moisture content of solids at various drying times. Further, Antony and Shyamkumar [15] observed the drying of sand particles in the FBD by studying the innumerable parameters of the velocity and temperature distribution of the inlet hot air.

However, achieving an ideal drying condition during the early stages of the experiment requires a high cost and a long drying time. Besides, development of the FBD system is also necessary as well some complications may hinder the accurate measurement of the parameters and ultimately affect the drying process. Due to lack of information regarding the requirements for achieving an ideal operation condition in the drying process, the computational fluid dynamics (CFD) simulation seem to provide more beneficial than conducting experiments since various factors and parameters can affect the operation conditions.

Thus, in this study, a model of a horizontal FBD was developed in the ANSYS© SpaceClaim 19.2 and a CFD simulation was performed in the ANSYS© Fluent 19.2 [16]. Prior to run the simulation, a mesh independent test has been conducted to evaluate the quality of the mesh that was generated by the FBD geometry. The CFD simulation was adopted in order to analyse the drying rate and observe the behaviour of fluidizing rate inside the FBD as the CFD can provide high-fidelity databases by diagnosing the flow field. In the CFD process, numerical methods and algorithm are applied in order to solve and analyse problems involving the fluid flow. A Euler-Euler multiphase model has been employed and a k-epsilon turbulent model is activated in the simulation. The relationship between a sago's drying rate was studied at several inlet air velocity and hot air temperature. The profile of the temperature, sago volume fraction and moisture content of sago inside the FBD was observed in order to determine the ideal condition for drying of the sago bagasse. The product of this dried sago bagasse will be used as the animal feed after go further for some additional nutrients. Therefore, this drying process is an important stage to inhibit any microbial development and quality decay as well for the storage handling.

2. Sago Industry in Malaysia

Figure 1 shows the process flow of a sago processing involving of the starch extraction from sago tree [7]. In Sarawak, the starch isolation process is mechanically done in the modern sago factory. Mostly, the process of making starch will undergo process like debarking, filtering, settling washing, drying and packaging. The sago extraction starts when the trees is cut and sent to factory or mill. Then, the debarking process takes place in the factory which will produce solid waste in the form of sago bark and sago bagasse. In the pulping process, sago chips are then crushed in a rotating drum fed continuously with water, and the resultant slurry sieved over a series of reciprocating screens to separate the starch 'milk' from the fibrous pulp. The wet starch is then sieved to separate the abrasive fibres. Additional purification is done inside separators to obtain pure starches. During starch extraction process, by-products were produced which are the bark of the trunk, fibrous pith residue (known as bagasse/hampas) and wastewater. This sago bagasse contains lignocellulose fibre as the by-product from the starch extraction of the pith. The bagasse production rate depends on the quality of the starch extraction process.

With a rapid growth of a sago plantation and sago starch production, large amount of a waste has been produced every year and thus it must be handled environmentally. Among the efforts to manage this solid waste or sago bagasse is by converting it into a high-value product such as animal feed. This conversion process will undergo various stages including pre-treatment process, compression process as well as drying process [7]. The drying procedure is very crucial step in order to inhibit microbial growth and quality degeneration also for the loading handling.

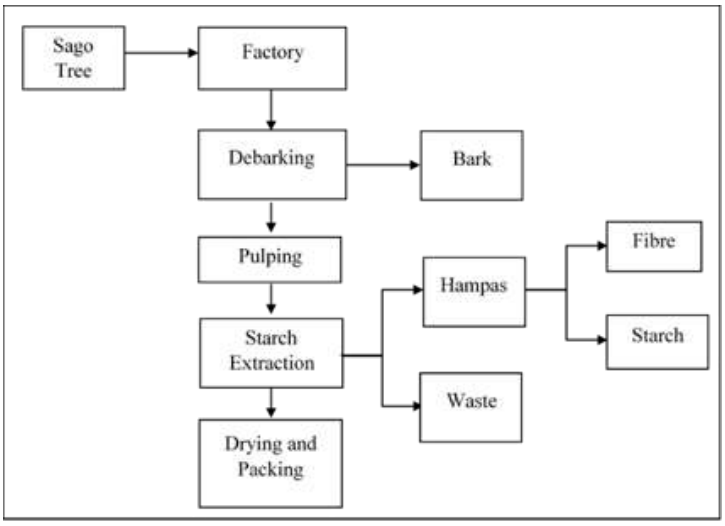

Fig. 1. Process flow of sago starch extraction from sago tree [7].

3. Computational Fluid Dynamics and Mathematical Modelling

Computational Fluid Dynamic (CFD) method is a system analysis method which involving the fluid flow, heat and mass transfer as well a phenomenon associated with the chemical reactions [16, 17]. This method is very dominant and covers a variety of uses industrial applications like thrust applications and forces in aerodynamic vehicles, hydropower dynamics for ships, combustion in engines and gas turbines, fluid flow in spin routes, cooling in microelectronic circuits, mixing and separation in a chemical engineering process. The CFD approach provides an understanding into the flow configurations which are challenging, costly or difficult to solve using some conventional experimental techniques [18]. Although the tools for applying single-phase CFD are extensively accessible, the application of a multiphase CFD is yet, still complex to solve in the physical and numerical method. Besides, the multiphase CFD simulations are time consuming as well as hence, a flow prediction in a bulky scale tools are not obtained readily.

Thus, in this study, two methodologies have been employed for modelling of multiphase fluid flow which is Euler-Lagrange and Euler-Euler method. The Euler-Euler method is widely used for modelling of a gas-solid flow and suitable for simulating larger and complex geometry of the industrial FBD, also it uses less computational power [16-19]. The conservation of mass, momentum and energy are applied as shows in the Eqs. (1) to (3) below in order to solve the Eulerian multiphase model which was developed based on Eulerian-Eulerian model, using an averaging approach [20, 21].

$$\frac{\delta}{\delta t}\left(\alpha_q \rho_g\right) + \nabla \cdot \left(\alpha_q \rho_g \vec{v_q}\right) = \sum_{p=0}^{n}\left(m_{pq} - m_{qp}\right) - S_q \tag{1}$$

$$\frac{\delta}{\delta t}\left(\varepsilon_s \rho_s\right) + \nabla \cdot \left(\varepsilon_s \rho_s v_s\right) = 0 \tag{2}$$

$$\frac{\delta}{\delta t}\left(\varepsilon \rho h\right) + \nabla \cdot \left(\varepsilon \rho v h_s\right) - \varepsilon \frac{\delta p}{\delta t} + \nabla \tau : \nabla \vec{v} - \nabla \vec{q} + Q_{gs} + m\Delta H_{vap} \tag{3}$$

where $\overrightarrow{v_q}$ is a velocity for q phase, p is a *p*ressure, $\dot{m}_{pq}$ is a mass transfer from p phase to q phase, $\dot{m}_{qp}$ is a mass transfer from q phase to p phase, h is a heat transfer coefficient, ρ is a density, q is a heat flux, ε is a volume fraction, Q is a heat transfer rate, v is a vector velocity, H is a latent heat and τ is a shear stress tensor.

By choosing the appropriate boundary conditions, the governing equations were solved. The first-order implicit was selected as it is considered adequate for the transient formulation in most problems [19]. In the spatial discretization, the first-order upwind was applied for the convective terms except for the momentum, while the second-order upwind was applied to increase the convergence.

4. Methodology

In the CFD process, the computation simulation required the input of the category of model, properties of the parameters on each boundary, and operating conditions. To solve the simulation problem, some assumptions are defined and the governing equations are formulated. The horizontal FBD model was developed by using ANSYS SpaceClaim© 19.2 software. The FBD model was designed based on the studied done by Mujumdar [9] and Mezhericher et al. [22] where the details dimensions are shown in a Table 1.

Table 1. FBD design dimension [9, 22].

	Diameter (mm)	Length (mm)
FBD main body	1400	4000
Outlet channel	200	200
Inlet hot air channel	60	50

4.1. Assumptions and boundary conditions

The CFD simulation was run in the ANSYS© Fluent 19.2 on *Intel i5* with 4 core processor Windows 10 and it takes more than 24 hours for each simulation to converged and completed. Table 2 shows the parameters and ANSYS© Fluent 19.2 setting for operating and boundary conditions specified in this simulation study [15, 19, 24]. In this study, based on the studied by Rosli et al. [19], six assumptions were made which are (i) the size of sago particles was set as 2000μm since this particle size can fluidize easily and it is the average size for sago bagasse in the industry [23], (ii) the incoming air velocity of the inlet supply is uniform, (iii) the physical and thermokinetic properties of sago are considered to be same as that of cassava, (iv) water content in the sago at the initial condition is 40% (w/w), (v) all the sago bagasse is already inside the FBD at the beginning of the simulation and (vi) all materials are well mixed in the FBD. Besides, the meshing analysis and a mesh independence test were then performed to evaluate the quality of mesh that were generated.

The simulation was performed with the air velocities of V=5, 8 and 10 ms^{-1} and at the temperatures of T=50, 70 and 100ºC. These values are selected that are representing the initial, middle and upper range of the parameter. Also, it was known that the sago particles exhibit good fluidization in the FBD at velocities between 1-10 ms^{-1} and at the temperatures between 50-100ºC as well are capable of producing a good drying pattern for particle size of 2000μm [19, 24].

Table 2. ANSYS© Fluent Setting [15, 19, 24].

Input setting	Variables / Parameters in ANSYS©	
Physics	Multiphase, Species Transport, Viscous Model, Energy	
Turbulent model	k-ε (Realizable)	
Iteration	20	
Phase type	Primary Secondary Tertiary	Air Sago bagasse Water
Time based study	Transient	
Solver scheme	Phase-coupled SIMPLE	
Boundary conditions	Particle size Initial water content in sago Turbulent intensity Wall condition	2000 µm 40 % (w/w) 5 % No Slip
Operating conditions	Air temperature Air velocity	50, 70, 100°C 5, 8, 10 ms^{-1}
Time step	500	
Step time size	0.01 s	

4.2. Mechanism and modelling of the fluidized bed dryer (FBD)

Fluidization can be defined as a process where there are contact between a solid and fluid that will be form a bed of solid particles which is elevated and agitated by a flow of rising fluid, thus creating this bed behaves like a fluid [25]. According to Antony and Shyamkumar 15], the process involved in the FBD is a convection heat transfer. The heated air passes to with the wet particles and will dry the suspended solid materials in the bed. This heated air will flow from the bottom to the top of the dryer that will fluidize the wet solid materials. During this process, the hot air will absorb the water content through the principle of heat transfer and remove it through the outlet. Thus, the FBD is designed to maximize the contact between sago bagasse with a hot air. A typical schematic diagram of a FBD is illustrated as shown in Fig. 2.

Typically, a FBD consists of a container or a chamber. A porous plate will be placed at the bottom of the chamber. There is also a plenum chamber that control the incoming air velocity and the hot air will draw into the chamber. The material which is in the form of moist granules will feed into the chamber before interacting with the hot air from the bottom side. The heated air will mix with the solid materials and form the lava-like layer that results in an efficient mix between the air and the material [12]. The combination of mechanical conveying and hot air stream along the FBD will remove the remaining moisture content. The mechanical conveyor will loosen the sago residues fibres, providing more contact areas with the hot air stream. Then, the dried product of the materials will be removed from the dryer via the outlet as it being transported by the mechanical conveyor and then collected and stored by the packaging unit.

For this simulation approach, the horizontal FBD model was successfully developed in the ANSYS© SpaceClaim 19.2 software based on the specification and dimension listed in Table 1. Figure 3(a) shows the details dimension of the

FBD model in the 2D view with the length of FBD is 4000 mm in the *x*-axis and its diameter is 1400 mm in the *y*-axis.

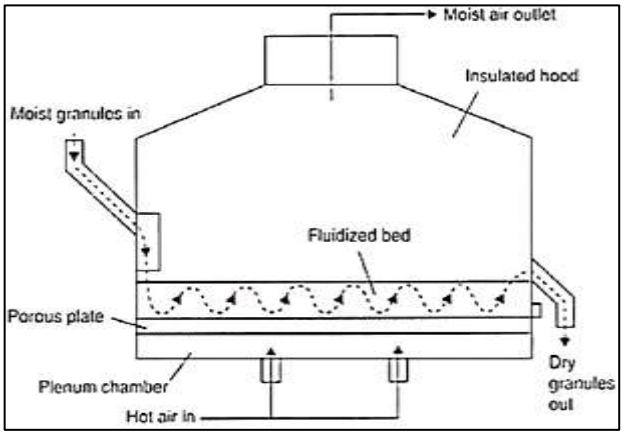

Fig. 2. Schematic diagram of a typical FBD [12].

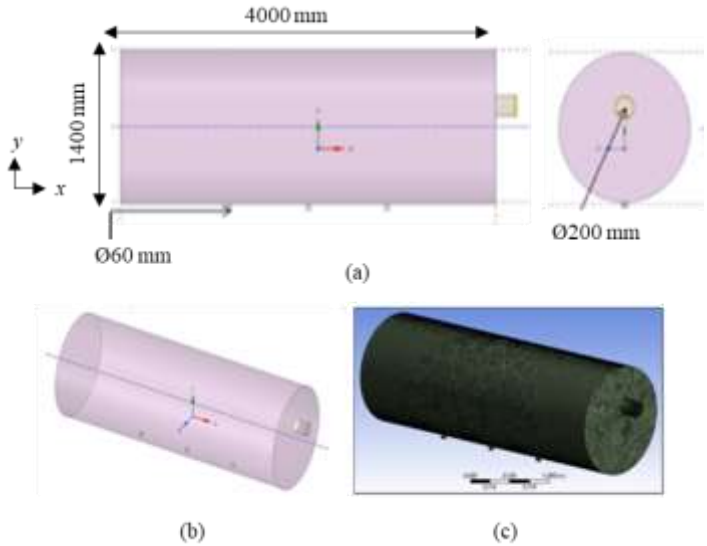

Fig. 3. FBD models with (a) details dimension of the FBD geometry (b) 3D FBD model created with ANSYS© SpaceClaim 19.2 and (c) FBD mesh generated with ANSYS© Meshing.

There are three inlets of the hot air supply at the bottom side with its diameter is 60 mm and one outlet at the right side. The left side in the Fig. 3(a) shows the front view of the FBD and the right side shows the side view with the diameter of the outlet is 200 mm. Fig. 3(b) shows an isometric 3D view of the FBD and Fig. 3(c) shows the meshing FBD that was done with ANSYS© Mesh. The local meshing is performed at three positions; inlet, outlet and the main body of FBD. This is to ensure that the mesh developed is refined enough at these positions before

the global mesh is generated. The mesh generated have a good quality with the value of the skewness quality is 0.20568 and the value of the orthogonal quality is 0.99504 which is a good quality.

5. Results and Discussions

In this simulation study, a temperature profile, a sago volume fraction in the FBD and a mass fraction of water in the sago bagasse are observed and determined at different inlet air velocities and temperatures.

5.1. Temperature profile in the FBD at different inlet air velocities

Figure 4 shows the temperature distribution profile inside the FBD at several inlet air velocities; V=5, 8 and 10 ms^{-1}. The colour bar represents the air temperature distribution inside the FBD where the red colour shows the maximum temperature distribution was achieved at 167^{o}C (440K) whereas the blue colour represents the minimum temperature distribution which almost nearly to 18^{o}C (291K).

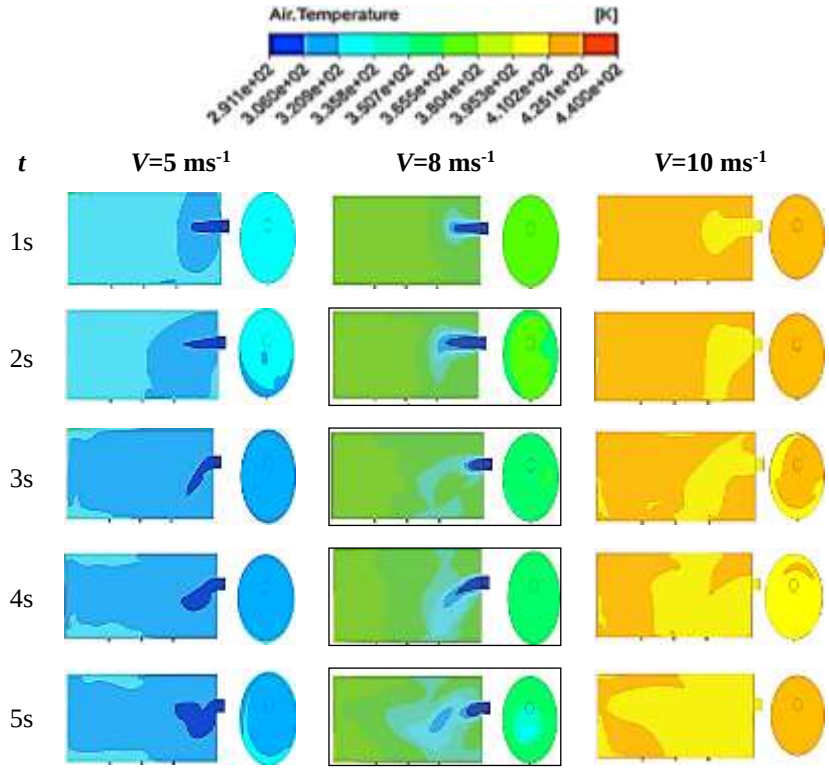

Fig. 4. Temperature profile in the FBD at three velocities; V=5, 8 and 10 ms^{-1} at t=1-5 s.

With the inlet air velocity of V=5 ms^{-1} supplied to the FBD, it shows that at the beginning of the simulation, the air temperature inside the FBD is 321K (50^{o}C) and after t=3 s, the temperature dropped to 306K. Observation at t=5s depicted that the temperature was nearly uniform inside the FBD with the lowest temperature

observed at the outlet stream of the FBD (right side). This is due to the water droplet in the sago bagasse's particle is being transported out of the FBD through the outlet area. As the air velocity increases, the temperature distribution inside the FBD is slightly increased up to 366 K and 425 K for V=8 ms^{-1} and V=10 ms^{-1}, respectively. This phenomenon is occurred as the heat transfer was took a place inside the FBD due to evaporation process occurred at the sago particle surface. This evaporation process is an endothermic reaction where it cools down the surrounding air inside the FBD. This observation of the temperature flow pattern is at agreement with the experimental work done by Okoronkwo et al. [26]. As the time elapsed, the temperature distribution inside the FBD was constant, implying that the drying process has occurred by reducing the water content in the sago bagasse. As well, it shows the feed of the inlet air with those velocities' ranges are sufficient to make the fluidization of the sago bagasse process in the designed FBD.

Besides, the temperature distribution inside the FBD was determined at various inlet air temperatures. Figure 5 shows the average temperature distribution inside the FBD at T=50, 70 and 100°C with V=5 ms^{-1}. The initial time (t=0 s) shows the starting point when the hot air is supplied to the FBD and it shows the temperature distribution inside the FBD is decreased as the drying time elapsed. For example, at the inlet temperature of T=100ºC, the temperature distribution inside the FBD dropped to T=81.5ºC, while, at T=70ºC, the temperature distribution dropped up to 62.5ºC. This result shows the cooling effect occurred in the FBD as a result of the endothermic reaction from the evaporation process of the water from the sago surface.

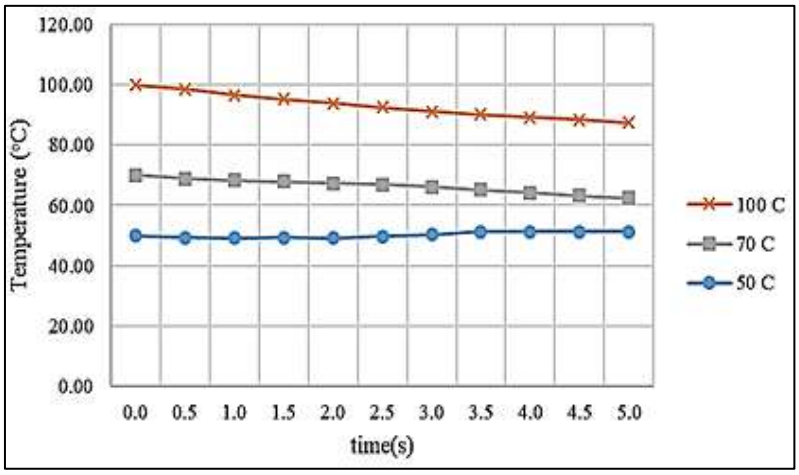

Fig. 5. Average temperature distribution inside the FBD at various inlet air temperature; T=50, 70 and 100°C with V=5 ms^{-1}.

In the evaporation process, the air heating increases the drying force for heat transfer and accelerates the drying process [9, 10]. It also reduces the air relative humidity, and further increases the driving force for drying. As the moisture content falls, the particle of the sago bagasse would heat up and higher temperatures speeds up the water diffusion from the interior of the sago particle to the surface. Thus, the air temperature in the FBD decreases during the drying process where the air temperature is uniformly distributed in the FBD.

However, for the inlet air temperature of T=50ºC, the temperature distribution in the FBD is quite unstable and it was obvious between T=50°C to 52.5°C. It shows at the lower air temperature, the evaporation process in the FBD was almost none and this implies that the sago particle should have a minimum fluidization velocity and air temperature in order for fluidization process takes place [9, 23, 27]. At the certain air velocity, the fluidization will occur when the inlet air can withstand the weight of the whole bed. This condition is called minimum fluidization and the corresponding velocity is named fluidization velocity (U_{mf}) [9, 10]. At this velocity, it will support the sago particle to fluidize as well to reduce the moisture content in the final sago bagasse. Thus, higher inlet temperatures of drying air should be met which leads to shorter drying times. However, the product quality considerations limit the applicable rise to the air temperature [9, 10, 24]. Excessive hot air can almost completely dehydrate the sago bagasse surface, making its pores to shrink and almost close, leading to crust formation or "case hardening", which is usually undesirable.

From this observation, it can be depicted that the drying temperature has play a significant effect on sago starch drying kinetic; thus, drying temperature would be the basis to select the ideal drying condition. In this study, the hot air temperature of T=70 ºC was chosen as the optimum temperature for sago drying. It was also supported with the studied by Mustafa Kamal et al. [28] where the temperature ranging from T=50 to 80ºC affected the product quality particularly in term of colour and the sago tends to be gelatinous if the temperature above 90ºC is applied.

5.2. Sago volume fraction in the FBD

Figure 6 shows 3D flow profile of the sago volume fraction in the FBD at T=70°C and V=10 ms^{-1} in 5 s time simulation. The colour bar represents the sago volume fraction in the final sago bagasse after the drying process where the red colour shows the highest sago fraction in the final sago bagasse with the value of 0.6. Whereas the blue colour shows the lowest sago fraction in the final sago bagasse with the value nearly to zero. The highest sago fraction in the FBD is 0.6 as the initial water content in the sago bagasse is 40% (v/v).

At the beginning of drying process (t=0 s) as shown in a Fig. 6(a), partial area of the FBD was covered by the maximum fraction of the sago bagasse which shown in the red color at the lower FBD area as the sago bagasse was assumed already inside the FBD at the beginning of the simulation process. The initial sago fraction is indicated at 0.6, however as the drying time took place, the water content in the sago mass fraction is slowly decreased as a result of the water loss from the sago particle through the evaporation process.

Besides, it shows the sago volume fraction in the FBD keep decreased at the center area of FBD. It shows the sago bagasse was fluidized inside the FBD with an existence of the hot air supply that increases the particle's movement and reduce the moisture content of the sago bagasse. From t=3.0 s, it can be seen that the fluidization process achieved the optimum condition where all the sago bagasse already being fluidized at the all areas inside of the FBD as shown in a Fig. 6(i) to Fig. 6(l). At the end of the drying process (t=5 s) as shown in a Fig. 6(l), the yellowish green colour indicated that most area of the FBD was covered with almost 0.4 of sago and 0.2 of water content. It shows the moisture content of the

sago bagasse was reduced from 40% (v/v) to 20% (v/v) after going through the drying process via the FBD.

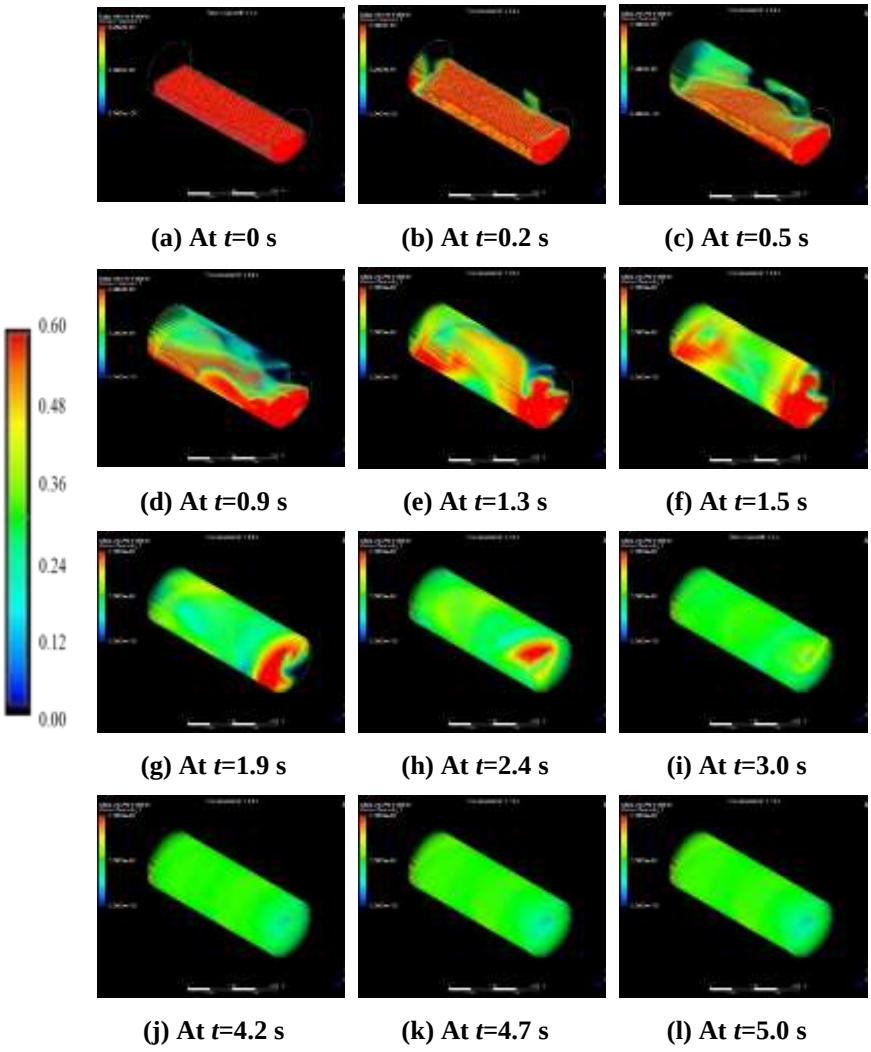

(a) At *t*=0 s **(b) At *t*=0.2 s** **(c) At *t*=0.5 s**

(d) At *t*=0.9 s **(e) At *t*=1.3 s** **(f) At *t*=1.5 s**

(g) At *t*=1.9 s **(h) At *t*=2.4 s** **(i) At *t*=3.0 s**

(j) At *t*=4.2 s **(k) At *t*=4.7 s** **(l) At *t*=5.0 s**

Fig. 6. 3D flow profile of sago volume fraction inside the FBD at *V*=10 ms^{-1} and T=70°C in 5s time simulation.

5.3. Mass fraction of water in the sago bagasse

From the previous studied [20, 22-25, 28], they found that the hot air temperature plays a significant role in the drying process. Thus, in order to determine the higher drying rate at the inlet temperature of T=50, 70 and 100°C, the relationship of the moisture content in the sago bagasse was studied. Fig. 7 shows the comparison of the mass fraction of water in the sago bagasse at V=10 ms^{-1} with various inlet air temperature. With the initial of water content in the sago is 40% (v/v), it shows the water content in the sago bagasse decreases with a time. At the inlet air temperature

of T=50ºC, the water mass fraction in the sago is decreased to 20.21%, whereas it was decreased to 17.79% and 15.70% at T=70ºC and T=100ºC, respectively.

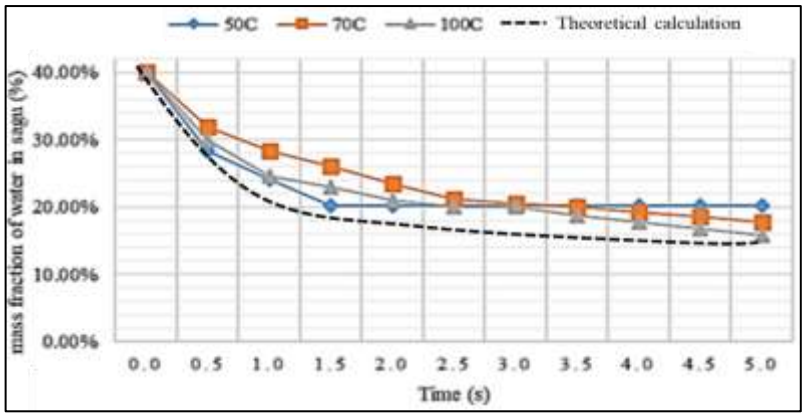

Fig. 7. Mass fraction of water in the sago bagasse at V=10 ms^{-1} with various inlet air temperature; T=50, 70 and 100°C.

From this result, the percentage of the water content reduction in the final sago bagasse can be determined. The water reduction is approximately at 19.8%, 22.3% and 24.3% for T=50, 80 and 100°C, respectively based on the total mass of 40%. It shows that at the higher inlet temperature, the losses of the water from the sago particle is higher where more water will be evaporated from the surface of particle sago. Therefore, the moisture content losses are proportional with the inlet air temperature [10].

Figure 7 also shows a comparison between theoretical findings [9, 15, 20, 24, 25, 29] and this study result of the moisture content versus time. This result can be divided into three sections where the first sudden drop section represents the constant-rate period [9, 10, 24]. In this section (at point of t=0-2 s), the moisture is considered to be evaporating from a saturated sago surface at a rate governed by diffusion from the surface through the stationary air film that is in contact with it. This period depends on the air temperature, humidity and speed of moisture to the surface, which in turn determines the temperature of the saturated sago surface. During the constant rate period, the water must be transported to the surface at a rate sufficient to maintain the saturation.

At the end of the constant rate period (at point of t=2 s), a break in the drying curve occurs. This point is called the critical moisture content, and a linear fall in the drying rate occurs with further drying. This section is called the first falling-rate period. As drying proceeds, moisture reaches the surface at a decreasing rate and the mechanism that controls its transfer will influence the rate of drying. Since the surface is no longer saturated, it will tend to rise above the wet bulb temperature. This section, represented at point of t=4 s in Fig. 7 is called the second falling-rate period, and is controlled by a vapor diffusion [9, 10]. Movement of liquid may occur by diffusion under the concentration gradient created by the depletion of water at the surface. The gradient can be caused by evaporation, or as a result of capillary forces, or through a cycle of vaporization and condensation, or by osmotic effects. As the overall, it can be said that this finding concludes that the hot air velocity and temperature play a

significant factor in the drying process where the higher temperature will heat up the fluidization bed and the velocity will accelerate the drying process. This resulted in the higher moisture diffusivity; hence the drying rate is also increased.

6. Conclusions

A horizontal FBD model was successfully developed in ANSYS© SpaceClaim 19.2 software. The multiphase CFD simulation is also successfully carried out by using Euler-Euler multiphase approach and employing the k-epsilon turbulent equation. Based on the results, it can be concluded that the inlet velocity and temperature play an important factor that will determine the drying rate of the final sago bagasse. The higher of the inlet temperature and velocity will result in the greater drying rate and shorter drying time. To achieve the shorter drying time in the FBD, the temperature of 70°C and hot air velocity of 10 ms^{-1} was found to be the optimum condition for sago drying. Besides, the temperature distribution flow profile is at a good agreement with the experimental where the drying rate of sago is proportional with the velocity and temperature. The final moisture content of the sago is able to be reduced from the initial value of 40% to 15.7% (v/v). This final value of the moisture content in the sago is in a good range in order for the sago bagasse to be converted into animal feed and also other high value products.

Nomenclatures

g	Gravity, ms^{-2}
H	Latent heat, Joule
h	Heat transfer coefficient, $Wm^{-2}K^{-1}$
$\dot{m}_{pq}$	Mass transfer from p phase to q phase, kgs^{-1}
$\dot{m}_{qp}$	Mass transfer from q phase to p phase, kgs^{-1}
p	Pressure, Nm^{-2}
Q	Heat transfer rate, Watt
q	Heat flux, Wm^{-2}

Greek Symbols

ε	Volume fraction
ρ	Density, kgm^{-3}
τ	Shear stress tensor, Pa
v	Vector velocity, ms^{-1}

Abbreviations

CFD	Computational Fluid Dynamic
FBD	Fluidized Bed Dryer

References

1. Naim, H.M.; Yaakub, A.N.; and Hamdan, D.A.A. (2016). Commercialization of sago through estate plantation scheme in Sarawak: The way forward. *International Journal of Agronomy*, Volume 2016, Article ID 8319542, 6 pages.
2. Pei-Lang, A.T.; Mohamed, A.M.D.; and Karim, A.A. (2006). Sago starch and composition of associated components in palms of different growth stages. *Carbohydrate Polymers*, 63(2), 283-286.

3. Karim, A.A.; Tie, A.P.L.; Manan, D.M.A.; and Zaidul, I.S.M. (2008). Starch from the sago (Metroxylon sagu) palm tree properties, prospects, and challenges as a new industrial source for food and other uses. *Comprehensive Reviews in Food Science and Food Safety*, 7(3), 215-228.
4. Metaragakusuma, A.P.; Katsuya, O.; and Bai, H. (2015). An overview of the traditional use of sago for sago based food industry in Indonesia. *ICoA Conference Proceedings*, 119-124.
5. Bujang, K.B. (2008). *Potentials of bioenergy from the sago industries in Malaysia*. Encyclopedia of Life Support System XIV.
6. Kadirvelu, K.; Kavipriya, M.; Karthika, C.; Vennilamani, N.; and Pattabhi, S. (2004). Mercury (II) adsorption by activated carbon made from sago waste. *Carbon*, 42(4), 745-752.
7. Awg-Adeni, D.S.; Abd-Aziz, S.; Bujang, K.; and Hassan, M.A. (2010). Bioconversion of sago residue into value added products. *African Journal of Biotechnology*, 9(14), 2016-2021.
8. Liestianty, D.; Rodianawati, I.; and Patimah, M. (2016). Chemical composition of modified and fortified sago starch (Metroxylonsp) from Northern Maluku. *International Journal of Applied Chemistry*, 12(3), 243-249.
9. Mujumdar, A. (1995). *Handbook of industrial drying* (2nd Ed.). Marcel Dekker Publishing.
10. Wan Daud, W.R. (2008). Fluidized bed dryers-recent advances. *Advanced Powder Technology*, 19(5), 403-418.
11. Zielinska, M.; and Markowski, M. (2007). Drying behavior of carrots dried in a spout-fluidized bed dryer. *Drying Technology*, 25(1), 261-270.
12. Sivakumar, R.; Saravanan, R.; Perumal, A.E.; and Iniyan, S. (2016). Fluidized bed drying of some agro products - A review. *Renewable and Sustainable Energy Reviews*, 61, 280-301.
13. Arumuganathan, T.; Manikantan, M.R.; Indurani, C.; Rai, R.D.; and Kamal, S. (2010). Texture and quality parameters of oyster mushroom as influenced by drying methods. *International Agrophysics*, 24, 339-342.
14. Mortier, S.T.F.C.; De Beer, T.; Remon, J.P.; VerVaet, C.; and Nopens, I. (2011). Mechanistic modelling of fluidized bed drying processes of wet porous granules: A review. *European Journal of Pharmaceutics and Biopharmaceutics*, 79(2), 205-225.
15. Antony, J.; and Shyamkumar, M.B. (2016). Study on sand particles drying in a fluidized bed dryer using CFD. *International Journal of Engineering Studies*, 8(2),129-145.
16. Ansys Inc. (2013). Ansys fluent in Ansys workbench user's guide. Ansys, Inc.
17. Versteeg, H.; and Malalasekera, W. (2007). *An introduction to computational fluid dynamics-The finite volume method* (2nd ed). Pearson-Prentice Hall.
18. Hamzehei, M. (2012). CFD modeling and simulation of hydrodynamics in fluidized bed dryer with experimental validation. ISRN Mechanical Engineering 10.5402/2011/131087.
19. Rosli, M.I.; Nasir, A.M.; Muim, A.; Takriff, M.S.; and Chern, L.P. (2018). Simulation of a fluidized bed dryer for the drying of sago waste. *Energies*, 11(9), 1-8.

20. Babu, A.K.; Kumaresan, G.; Raj, V.A.A.; and Velraj, R. (2018). Review of leaf drying: Mechanism and influencing parameters, drying methods, nutrient preservation, and mathematical models. *Renewable and Sustainable Energy Review*, 90, 536-556.
21. Argyropoulos, C.D.; and Markatos, N.C. (2015). Recent advances on the numerical modelling of turbulent flows. *Applied Mathematical Modelling*, 39(2), 693-732.
22. Mezhericher, M.; Levy, A.; and Borde, I. (2007). Theoretical drying model of single droplets containing insoluble or dissolved solids. *Dry Technology*, 25(6), 1025-1032.
23. Geldart, D. (1972). The effect of particle size and size distribution on the behaviour of gas-fluidised beds. *Powder Technology*, 6(4), 201-215.
24. Tasirin, S.M.; Kamarudin, S.K.; Jaafar, K.; and Lee, K.F. (2007). The drying kinetics of bird's chillies in a fluidized bed dryer. *Journal of Food Engineering*, 79(2), 695-705
25. Oluwaleye, I.O.; and Adeyemi, M.B. (2013). Experimental evaluation of a batch hot air fluidized bed dryer. *International Journal of Modern Engineering Research* (*IJMER*), 3(1), 497-503.
26. Orokonkwo, C.A.; Nwufo, O.C.; Nwaigwe, K.N.; Oguuke, N.V.; and Anyanmwu, E. (2013). Experimental evaluation of a fluidized bed dryer performance. *The International Journal of Engineering and Science*, 2(6), 45-53.
27. Sahni, E.K.; and Chaudhuri, B. (2012). Contact drying: A review of experimental and mechanistic modeling approaches. *International Journal of Pharmaceutics*, 434(1-2), 334-348.
28. Mustafa Kamal, M.; Baini, R; Mohamaddan, S.; Selaman, O.S.; Ahmad Zauzi, N.; Rahman, M.R.; Abdul Rahman, N.; Chong, K.H.; Atan, M.F.; Abdul Samat, N.A.S.; Taib, S.N.L.; and Othman, A.K. (2017). Effect of temperature to the properties of sago starch. *IOP Conference Series: Materials Science and Engineering*, 206, 1-14.
29. Mujumdar, A.S. (2014). *Handbook of industrial drying*, (4th ed). Taylor & Francis Group.